

Technical Note

Use of Multicoil Arrays for Separation of Signal from Multiple Slices Simultaneously Excited

David J. Larkman, PhD,^{1*} Joseph V. Hajnal, PhD,¹ Amy H. Herlihy, PhD,¹
Glyn A. Coutts, PhD,¹ Ian R. Young, PhD,¹ and Gösta Ehnholm, PhD²

Increased acquisition efficiency has been achieved by exciting several slices simultaneously. The mixed data were unfolded to produce separate slices using the spatial encoding information inherent in a multicoil receiver system. Each coil yields a linear combination of signals from all excited slices weighted by the sensitivity of each coil. A matrix inversion provides a solution to unfold these images. J. Magn. Reson. Imaging 2001;13:313–317. © 2001 Wiley-Liss, Inc.

Index terms: fast-imaging; simultaneous excitation; multi-slice; phased-array

OPTIMISING SPEED of image acquisition is an important consideration in *in vivo* MRI, both to reduce patient examination time and/or to increase temporal resolution in dynamic studies. Most fast acquisition schemes [echoplanar imaging (EPI), fast spin echo (FSE), etc.] have unique contrast properties different from the slower standard sequences from which they evolved. Traditional multislice MRI is reliant on radiofrequency (RF) excitation of single slices that are then detected with one or more receive coils. This can then be repeated or interleaved to acquire a block of slices. Here we have simultaneously excited multiple slices and untangled the resultant mixed images, using a multi-detector array and receive system. Previous attempts to make use of simultaneous multislice acquisitions have relied on encoding unique phase information into each slice position (1,2). This generally requires multiple excitations to achieve slice differentiation.

An alternative approach is demonstrated here. Each receive channel yields a linear combination of signals from all excited slices modulated by the individual coil sensitivities. The slice data can be untangled using matrix algebra to solve a set of simultaneous complex linear equations. This requires prior knowledge of the spatially dependent coil sensitivity. Other related tech-

niques have been developed for reducing the number of phase-encode steps in spin wrap imaging by using multiple coils (3–6). An allied approach has been developed that uses the sensitivity profile of the array coils to encode information in the Fourier domain. This technique is called simultaneous acquisition of spatial harmonics (SMASH) (7) and is applicable when the spatial distributions of coil sensitivities can be combined so as to closely resemble a series of sinusoids. The SMASH method operates in the Fourier domain and so is not directly applicable to the case of direct simultaneous excitation of distinct slices considered here.

THEORY

A multifrequency excitation (hence multislice in the spatial domain) can be constructed in several ways. Here we apply simple Fourier transform theory. We may start with a single slice pulse that is a digitally sampled RF profile with a frequency composition that reflects the desired slice profile, for example, an apodized sinc profile in the time domain, which transforms to a “box” profile in the frequency domain. Sinusoidal modulation of the pulse in the time domain produces a symmetric frequency offset in the frequency domain, creating a two-slice pulse. Repeating this with a higher frequency component produces four slices. Any even number of slices can be produced in this way provided the Nyquist criterion is satisfied by the digital sampling rate. The time domain form of a four-slice sinc pulse $f(t)$ is:

$$f(t) = A \frac{\sin(at)\cos(bt)\cos(2bt)}{at}, \quad -T/2 < t < T/2 \quad (1)$$

where A is an amplitude scaling factor, a gives the slice width and $2b$ the slice separation, and T is the length of the pulse. An apodization term may be required to avoid truncation artifact. Both 90° and 180° pulses can be designed in this way so field echo, spin echo, inversion recovery, and all other common acquisition techniques can be used.

Data are collected from such multiexcitation sequences in the usual way, and the technique is independent of the type of readout. The individual data channels are reconstructed separately so that as many

¹The Robert Steiner Magnetic Resonance Imaging Unit, Imperial College School of Medicine, Hammersmith Hospital, London W12 0HS, United Kingdom.

²Pickering Nordstar, Helsinki, Finland.

Presented at the ISMRM Annual Meeting, Philadelphia, 1999.

*Address reprint requests to: D.J.L., The Robert Steiner MRI Unit, Imperial College, Hammersmith Hospital Campus, Du Cane Road, London W12 0HS, UK.

Received January 20, 2000; Accepted August 10, 2000.

images as there are coils are produced. Each of these images contains information from all slice positions.

The simultaneously excited slices can be separated providing there is a minimum of the same number of coils as slices and each coil has a different complex sensitivity to any given slice. This sensitivity is spatially dependent, and for n slices with m coils the total complex signal acquired in coil i in a single pixel (C_i) is given by the equation:

$$S_{i1}x_1 + S_{i2}x_2 + S_{i3}x_3 + S_{ij}x_j \dots + S_{im}x_m = C_i \quad (2)$$

where S_{ij} is the complex sensitivity of coil i to slice j , and x_j is the spatially dependent complex signal from slice j . Similar expressions for the other coils can be constructed leading to a set of equations expressed in matrix form:

$$\begin{bmatrix} S_{11} & S_{12} & S_{13} & \dots & S_{1m} \\ S_{21} & S_{22} & S_{23} & \dots & S_{24} \\ S_{31} & S_{32} & S_{33} & \dots & S_{34} \\ \vdots & \vdots & \vdots & \dots & \vdots \\ S_{n1} & S_{n2} & S_{n3} & \dots & S_{nm} \end{bmatrix} \cdot \begin{bmatrix} x_1 \\ x_2 \\ x_3 \\ \vdots \\ x_n \end{bmatrix} = \begin{bmatrix} C_1 \\ C_2 \\ C_3 \\ \vdots \\ C_m \end{bmatrix} \quad (3)$$

and in shorthand notation:

$$[S] \cdot [x] = [C] \quad (4)$$

The solution for $[x]$ is given by:

$$[x] = [S]^{-1} \cdot [C] \quad (5)$$

where $[S]^{-1}$ is the inverse of the complex sensitivity matrix $[S]$. Provided $[S]$ is nonsingular, the set of complex matrices $[x]$ holds the MR signal at each pixel for each slice.

MATERIALS AND METHODS

The simultaneous excitation method was implemented on a 0.5-T Apollo scanner (Marconi Medical Systems,

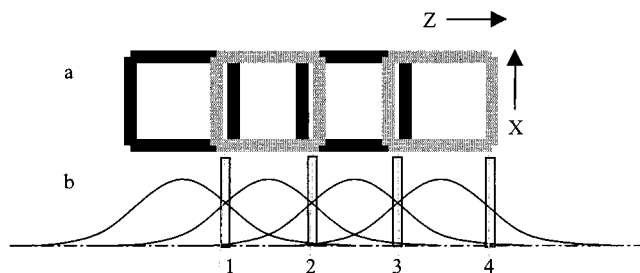


Figure 1. a: Schematic of the coil configuration showing the four overlapping surface coils. The arrows indicate the X and Z directions within the magnet. b: Magnitude sensitivity profiles for the coils at their center line and slice locations (1, 2, 3, 4). The coils are 120×120 mm². The slices are 100 mm apart, and their positions have been chosen such that the magnitudes of the sensitivities of nearest neighbor coils are approximately equal. This was the configuration used for the in vivo data; for the phantom data, the slice positions were moved 50 mm in the $-Z$ direction.

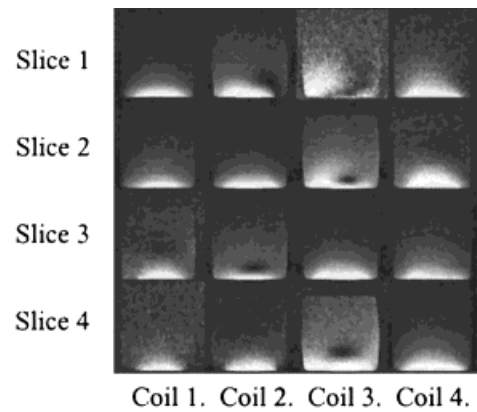
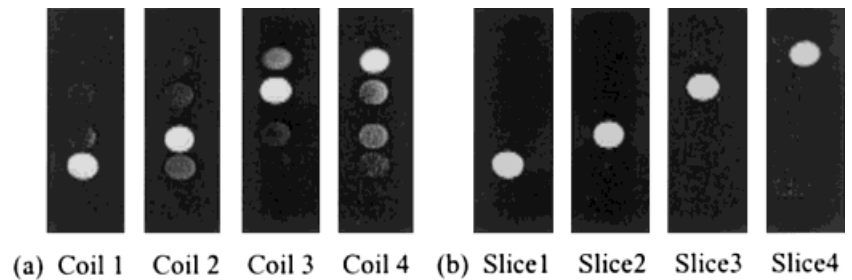


Figure 2. Image of the magnitude of the array sensitivity matrix. For each pixel there is a 4×4 matrix of complex elements. The data were obtained by imaging a large uniform phantom and consist of 16 magnitude images, one from each coil at each slice position.

Cleveland, OH) using a four-receive coil linear spine array (Fig. 1a). The spacing of the excited slices was commensurate with the coil spacing, but this is not a methodologic requirement. The complex sensitivity matrix was generated empirically from four reference acquisitions. Each reference acquisition excited a single transverse slice in a large uniform phantom, one at each of the four positions at which the multislice excitation operated. These data then contain the sensitivity of each coil to a single slice at each position, and this information provides the complex 4×4 array ($[S]$ in Eq. [4]) for each pixel within the area covered by the uniform phantom. These data need only be acquired once for a fixed geometry of coils and slices. Figure 2 shows the array sensitivity matrix $[S]$ in Eq. [5]. It is not necessary that the sensitivity matrix data and the image data be acquired with the same sequence or the same sequence parameters, as the sensitivity is only a function of the imaging coil and field used within a tolerance defined by coil loading effects. The sensitivity data may also be acquired during or after examination. They can be used to update or provide verification of the initial acquisition. For the coil in this study the sensitivity is slowly varying function in space, and so some tolerance to precise slice positioning is inherent; however, mapping the sensitivity profiles for each examination where this technique is used is recommended. In the example presented, the sensitivity matrix acquisitions had the same sequence timing as the multislice acquisitions but with standard RF pulses.

Full simultaneous four-slice data were acquired with four cylindrical samples (length 9.0 cm and diameter 2.5 cm), one placed at each of the four slice positions. (The slice positions calculated from Eq. [1] were verified for the modified pulses prior to experiment, using a pyramid-shaped slice locating phantom.) The slice positions were at the center of the coils shown in Fig. 1a. They correspond to the peaks of the magnitude intensity profiles shown in Fig. 1b. This presents the unfolding algorithm with an intuitively optimal case where the difference in the magnitude of the sensitivity of nearest neighbor coils is maximum. A field echo sequence,

Figure 3. Images of four cylindrical phantoms that were placed with one centered at each slice position in Z and offset in X . The resultant magnitude images are shown before correction (a) and after correction (b).



128×256 matrix, was used with a field of view of 26 cm, TR/TE 400/8.1 msec, 2 sample averages, and total acquisition time 102 seconds. The slices were 100 mm from center to center and 10 mm thick. In vivo data were acquired from the leg of a consenting volunteer. The slice positions were at the positions shown in Fig. 1b, corresponding to the crossing points of the magnitude intensity profiles. This presents the unfolding algorithm with a more difficult case where the difference in the magnitude of the sensitivity of nearest neighbor coils is minimum. A spin-echo sequence, 128×256 matrix, was used with a field of view of 26 cm, TR/TE 400/8.1 msec, 2 sample averages, and total acquisition time 102 seconds. The slices were 100 mm from center to center and 10 mm thick.

The inverse complex sensitivity matrix for each pixel was calculated using Gaussian elimination, which was sufficient for this well-conditioned configuration in this application. In more challenging geometries, it is predicted that better results could be obtained using methods such as singular value decomposition: nonsingular values can be set to zero, for better conditioning of the matrix inversion. All image manipulations were performed using IDL (Research Systems, Boulder, CO) running on a DEC Alpha workstation.

RESULTS

Uncorrected magnitude images of the test phantoms from a four-slice simultaneously acquired data set can be seen in Fig. 3a (coils 1–4). Pixel by pixel corrected magnitude images are shown in Fig. 3b (slices 1–4). The uncorrected images show the mixed data (the magnitude of array $[C]$), and the corrected images have appropriately redistributed data (magnitude of array $[x]$). Both sets of images have been windowed and levelled in the same way. Figure 4 shows a single line profile through the magnitude image acquired by coil 4 (a,

before correction, and b, slice 4, after correction). Uncorrected and corrected magnitude images of the leg data can be seen in Fig. 5. The corrected images have been thresholded on the determinant of the sensitivity matrix to exclude the areas outside the uniform phantom image used for the sensitivity matrix, where there is no information on coil sensitivities. (The extent of the phantom data can be seen from inspection of a single element in Fig. 2. By the nature of this correction technique, an intensity normalization of the images occurs. This is manifest in Fig. 5 as a surface coil sensitivity compensation in the corrected image.

DISCUSSION

We have demonstrated a technique for resolving four slice images with a four-coil array. For n coils the principle holds for $\leq n$ slices. A limitation is that each coil must have sufficiently different complex sensitivity to each slice for the matrix in Eq. [3] not to become ill conditioned. The condition for failure is related to the noise in the sensitivity matrix. Where the sensitivity to 2 pixels differs by less than the standard deviation of the noise, they are indistinguishable. For the principle to be generally useful, the whole volume of coil sensitivity can be mapped. Once this is done, oblique slices in any orientation that satisfies the above criteria can be resolved, assuming the coil geometry is fixed. We have found that this type of encoding can unfold slices even in the coronal plane, provided they still lie within the sensitivity of the coils.

This approach is limited, however, by effects of coil loading, which may cause the spatial sensitivity to differ for the acquisition of the sensitivity matrix and the acquisition of the image data. At 0.5 T, where coils in the array generally are lightly loaded by the patient, this problem is small. However, at higher fields (8), an appropriate correction may be needed. An-

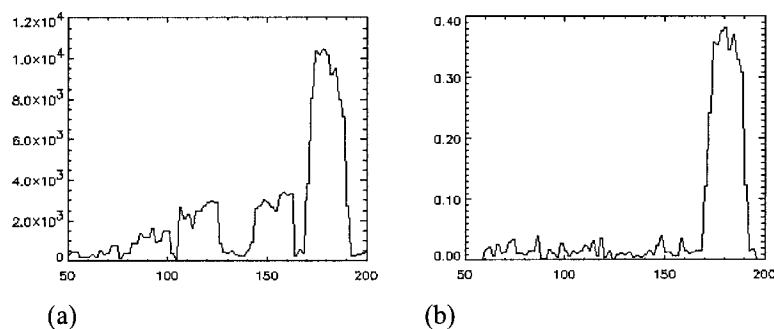


Figure 4. a: A single line of data (read direction) from coil 4, Fig. 4. b: The corresponding line from slice 4 after correction. The x axis units are pixels. The y axis is un-normalised arbitrary intensity.

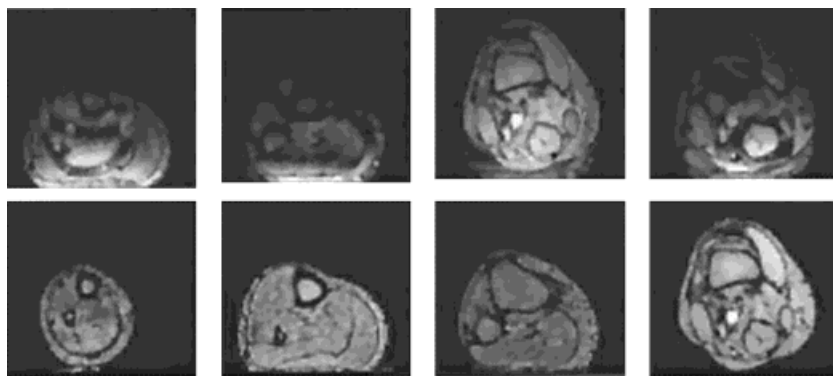


Figure 5. Images of a volunteer's leg; uncorrected coil images (top row) and corrected slice images (bottom row). The area to be corrected was selected by thresholding on the magnitude of the determinant of the sensitivity matrix shown in Fig. 2. These corrected images are normalized, which is manifest as a surface coil correction in these data.

other approach is to acquire sensitivity data with the subject in situ (9). This can ensure correct spatial registration of the sensitivity data and the image data, although difficulties can be encountered at the edges of anatomy if scan to scan motion of the subject is gross or motion artifact corrupts sensitivity information. Constant coil load conditions are satisfied in this case, but extra acquisitions are required during the patient examination.

By the nature of this correction technique an intensity normalization of the images occurs. If a matrix is multiplied by its inverse, the result is unity, because the signal intensity in the images to be corrected is of the same order as signal in the sensitivity matrix the final image is normalized to around one. This can clearly be seen in the corrected leg images shown in Fig. 5. The normalization manifests as a form of surface coil correction in these images where areas close to the coil have similar intensity (but greater signal-to-noise ratio [SNR]) than areas far from the coil. Since the process compensates solely for the sensitivity profile of the coils, it preserves the intrinsic tissue contrast provided by the imaging sequence.

Noise in such processing has two main detrimental contributions. Noise is critically dependent on the noise in the array sensitivity matrix $[S]$. The method relies on the use of a sensitivity matrix that is inherently noisy as it is obtained empirically. Any noise in this matrix is ultimately folded into the corrected data. The magnitude of this contribution depends on the noise level in individual receivers and the magnitude of their contribution to the unfolding in a given pixel. It is possible to eliminate the effects of this noise by smoothing the sensitivity data, as it consists primarily of slowly varying spatial frequencies (6). Local surface fitting, theoretical modeling of the sensitivity of such a coil, or a hybrid solution where empirical data are fitted to a parameterized model could also be useful approaches. There is then no noise contribution from the sensitivity matrix, but there is potential for systematic error resulting in nonperfect unfolding (residual ghosting in the image). The hybrid approach may hold the most promise, as it allows corrections for coil loading to be made while a statistically pure solution is maintained. The second noise source is intrinsic to the inversion solution. A given pixel is corrected by the addition or subtraction of the signal in 3 other pixels, one in each of the other

slices. These terms are modulated by the sensitivity information but nevertheless contain information with finite SNR. The combination of these terms produces a net noise gain that is coil geometry dependent.

Analysis of this noise is discussed in relation to phase-encode reduction sensitivity encoding in the literature (6). However, in the case of multislice encoding, there is no intrinsic reduction in SNR due to reduced scan time. Nonuniform data (ie, anatomic images) can be used to generate the sensitivity map (6). This approach has involved the addition of a further image acquisition stage using a coil with uniform sensitivity over the whole field of view (ie, the body coil on most MR instruments); here coil loading issues are avoided, and the accuracy of the technique is improved. However, additional processing of such images is required to remove this unwanted anatomic content, and care must be taken to extrapolate sensitivity information to a region outside the bounds of the subject to tolerate patient movement throughout the acquisition.

The principal application of the technique lies in the factor of n saving in acquisition time for n slices. Contrast-enhanced dynamic scanning, in which temporal resolution is paramount, would benefit directly from such an approach. We routinely use such array coils for endocavity applications (10). Spine imaging, for which coil arrays are routinely used, would benefit from shorter total acquisition times. Single-voxel MR spectroscopy may also benefit from these methods, with the ability to collect from multiple sites simultaneously rather than using multiple TRs for voxel differentiation. This allows for more data averaging and so greater tolerance of subject motion. Another application involves the elimination of foldover image contamination due to field and/or gradient inhomogeneity (11). Foldover artifacts arise when the same imaging frequency occurs both at a desired location within a slice and at another location. This is analogous to a two-slice excitation. The soluble degeneracy of this technique does not need to be all in the same direction. A combination of this multislice approach and one of the reduced phase-encode techniques SENSE (6) or SMASH (7) with an appropriate coil set could increase efficiency further.

REFERENCES

1. Souza SP, Szumowski J, Dumoulin CL, Plewes DP, Glover G. SIMA: simultaneous multislice acquisition of MR images by Hadamard-encoded excitation. *J Comput Assist Tomogr* 1988;12:1026-1030.
2. Muller S. Multifrequency selective RF pulses for multislice MR imaging. *Magn Reson Med* 1988;6:364-371.
3. Ra JB, Rim CY. Fast imaging using subencoding data sets from multiple detectors. *Magn Reson Med* 1993;30:142-145.
4. Hutchinson M, Raff U. Fast MRI data acquisition using multiple detectors. *Magn Reson Med* 1988;6:87-91.
5. Kwiat D, Einav S, Navon G. A decoupled coil detector array for fast image acquisition in magnetic resonance imaging. *Med Phys* 1991;18:251-265.
6. Pruessmann KP, Weiger M, Scheidegger MB, Boesiger P. Coil sensitivity encoding for fast MRI. In: *Proceedings of the ISRM Annual Meeting*, 1998. p 579.
7. Sodickson DK, Manning WJ. Simultaneous acquisition of spatial harmonics (SMASH): fast imaging with radiofrequency coil arrays. *Magn Reson Med* 1997;38:591-603.
8. Edelstein WA, Glover GH, Hardy CJ, Redington RW. The intrinsic signal-to-noise ratio in NMR imaging. *Magn Reson Med* 1986;3:604-618.
9. Pruessmann KP, Weiger M, Scheidegger MB, Boesiger P. SENSE: sensitivity encoding for fast MRI. *Magn Reson Med* 1999;42:952-962.
10. Gilderdale DJ, deSouza NM, Coutts GA, et al. Design and use of internal receiver coils for magnetic resonance imaging. *Br J Radiol* 1999;72:1141-1151.
11. Larkman DJ, Herlihy AH, Haganl JV. Elimination of gradient roll-over artefacts in MR images. *Radiology (Suppl)* 1999;213:232.